



Magnetoresistance of galfenol-based magnetic tunnel junction

Benoit Gobaut, G. Vinai, C. Castán-Guerrero, D. Krizmancic, H. Rafaqat, S. Roddaro, G. Rossi, G. Panaccione, Mahmoud Eddrief, Massimiliano Marangolo, et al.

► To cite this version:

Benoit Gobaut, G. Vinai, C. Castán-Guerrero, D. Krizmancic, H. Rafaqat, et al.. Magnetoresistance of galfenol-based magnetic tunnel junction. AIP Advances, 2015, 5 (12), pp.127128. 10.1063/1.4939019 . hal-01264418

HAL Id: hal-01264418

<https://hal.sorbonne-universite.fr/hal-01264418>

Submitted on 29 Jan 2016

HAL is a multi-disciplinary open access archive for the deposit and dissemination of scientific research documents, whether they are published or not. The documents may come from teaching and research institutions in France or abroad, or from public or private research centers.

L'archive ouverte pluridisciplinaire **HAL**, est destinée au dépôt et à la diffusion de documents scientifiques de niveau recherche, publiés ou non, émanant des établissements d'enseignement et de recherche français ou étrangers, des laboratoires publics ou privés.



Distributed under a Creative Commons Attribution 4.0 International License



Magnetoresistance of galfenol-based magnetic tunnel junction

B. Gobaut, G. Vinai, C. Castán-Guerrero, D. Krizmancic, H. Razaqat, S. Roddaro, G. Rossi, G. Panaccione, M. Eddrief, M. Marangolo, and P. Torelli

Citation: *AIP Advances* **5**, 127128 (2015); doi: 10.1063/1.4939019

View online: <http://dx.doi.org/10.1063/1.4939019>

View Table of Contents: <http://scitation.aip.org/content/aip/journal/adva/5/12?ver=pdfcov>

Published by the *AIP Publishing*

Articles you may be interested in

[Modelling the quasistatic and dynamical sensing response of Galfenol-based magnetostrictive devices](#)
Appl. Phys. Lett. **95**, 072504 (2009); 10.1063/1.3210789

[Magnetoresistance in Co/Pt based magnetic tunnel junctions with out-of-plane magnetization](#)
J. Appl. Phys. **103**, 07A918 (2008); 10.1063/1.2838282

[Giant magnetoresistance and tunnel magnetoresistance effects in FeCoGd-based spin valves and magnetic tunnel junctions](#)
J. Appl. Phys. **103**, 07F305 (2008); 10.1063/1.2830019

[Sign of tunneling magnetoresistance in Cr O₂-based magnetic tunnel junctions](#)
Appl. Phys. Lett. **91**, 252506 (2007); 10.1063/1.2825475

[Inverse magnetoresistance in chromium-dioxide-based magnetic tunnel junctions](#)
Appl. Phys. Lett. **78**, 1894 (2001); 10.1063/1.1356726

The image shows the cover of an AIP Applied Physics Reviews journal. It features a blue and orange color scheme with a molecular structure background. The text 'NEW Special Topic Sections' is prominently displayed in white. Below it, 'NOW ONLINE' is written in orange, followed by 'Lithium Niobate Properties and Applications: Reviews of Emerging Trends' in white. The AIP Applied Physics Reviews logo is in the bottom right corner.

NEW Special Topic Sections

NOW ONLINE
Lithium Niobate Properties and Applications:
Reviews of Emerging Trends

AIP Applied Physics Reviews

Magnetoresistance of galfenol-based magnetic tunnel junction

B. Gobaut,^{1,a} G. Vinai,² C. Castán-Guerrero,² D. Krizmancic,² H. Rafaqat,^{2,3}
 S. Roddaro,^{2,4} G. Rossi,^{2,5} G. Panaccione,² M. Eddrief,⁶ M. Marangolo,⁶
 and P. Torelli²

¹Sincrotrone Trieste S.C.p.A., S.S. 14 Km 163.5, Area Science Park, 34149 Trieste, Italy

²Laboratorio TASC, IOM-CNR, S.S. 14km 163.5, Basovizza, 34149 Trieste, Italy

³ICTP, Trieste, Italy

⁴NEST, Scuola Normale Superiore and Istituto Nanoscienze-CNR, Piazza S. Silvestro 12, 56127 Pisa, Italy

⁵Dipartimento di Fisica, Università di Milano, via Celoria 16, 20133 Milano, Italy

⁶Sorbonne Universités, UPMC Paris 06, CNRS-UMR 7588, Institut des Nanosciences de Paris, 75005, Paris, France

(Received 19 August 2015; accepted 11 December 2015; published online 21 December 2015)

The manipulation of ferromagnetic layer magnetization via electrical pulse is driving an intense research due to the important applications that this result will have on memory devices and sensors. In this study we realized a magnetotunnel junction in which one layer is made of Galfenol ($\text{Fe}_{1-x}\text{Ga}_x$) which possesses one of the highest magnetostrictive coefficient known. The multilayer stack has been grown by molecular beam epitaxy and e-beam evaporation. Optical lithography and physical etching have been combined to obtain 20x20 micron sized pillars. The obtained structures show tunneling conductivity across the junction and a tunnel magnetoresistance (TMR) effect of up to 11.5% in amplitude. © 2015 Author(s). All article content, except where otherwise noted, is licensed under a Creative Commons Attribution 3.0 Unported License. [<http://dx.doi.org/10.1063/1.4939019>]

INTRODUCTION

The effort for controlling the magnetization of ferromagnetic thin films by means of electric pulses has been tremendously intense in recent years.¹⁻³ This research was driven from the great potential applications that such a possibility would open in the domain of magnetic memories and sensors. In fact until now the magnetization direction has been controlled via dipole field or spin polarized currents; with respect to these means the magnetization switching via an electric pulse⁴ would reduce dramatically the energy consumption and/or the speed of the process. To obtain this result the research is moving in different directions⁵: find a material in which the magnetoelectric coupling is strong enough, the so-called multiferroics,^{6,7} to couple in suitable heterostructure ferroelectric and ferromagnetic layers^{8,9} (FE/FM) or to exploit the magnetoelastic coupling in piezoelectric/magnetostrictive junctions^{10,11} (PE/MS). While the bulk multiferroic materials, until now, have not shown satisfactory performances in terms of Curie temperature or total magnetization,¹² the FE/FM or the PE/MS heterojunctions have shown promising results and seem to be a viable solution to realize electrically controlled magnetization devices. The ideal experiment would be to change the resistive state of a magnetic tunnel junction (MTJ) via the application of an electric pulse. However prior to achieve this goal, it is mandatory to produce a working MTJ in which one layer presents a huge magnetostrictive coefficient¹³⁻¹⁵ and significantly different from the second magnetic layer.

We have prepared a device based on a piezoelectric/magnetostrictive junction with the simplest possible structure by substituting one of the FM layers of a Fe/MgO/Fe junction with a layer of magnetostrictive material (Galfenol). Indeed, Galfenol is now becoming a material of interest in the

^aCorresponding author: benoit.gobaut@elettra.eu

framework of spintronic^{16,17} thanks to its specific properties¹⁸ (high magnetostrictive coefficient for a material out of the rare-earth compounds, low coercive field, high Curie temperature). On another side, Fe/MgO/Fe heterostructure is known to exhibit a very high magnetoresistance ratio¹⁹ at room temperature, thus the obtained structure $\text{Fe}_{1-x}\text{Ga}_x/\text{MgO}/\text{Fe}$ appears to be ideal to test the coupling between the stress of the magnetostrictive material (Galfenol) and the resistance of the whole junction. Such a structure, combined with a piezoelectric substrate, could be the building block of a piezoelectricity-assisted TMR junction where the two resistance states (parallel (P) and antiparallel (AP) states) are obtained by applying an electric field. However, the high values of the TMR ratio in Fe/MgO/Fe junctions, compared to other layered structures, arise from the fact that the MgO crystalline barrier acts as a spin filter²⁰ particularly efficient for Fe electrodes due to coherent tunneling of fully spin-polarized Δ_1 electrons.^{21,22} Therefore, it is not straightforward to achieve a working MTJ device with this $\text{Fe}_{1-x}\text{Ga}_x/\text{MgO}/\text{Fe}$ stack because, the addition of Ga in the top Fe layer may strongly influence the electronic structure of this material and the coherency of the tunneling effect through the MgO barrier, thus affecting the magnetoresistance of the whole structure.

Here we describe the experimental realization of this device and report the observation of a magnetoresistive effect in it.

GROWTH, PATTERNING AND EXPERIMENTAL CONDITIONS

We have prepared a heterostructure of $\text{Fe}_{0.8}\text{Ga}_{0.2}$ (20 nm) /MgO(2.5 nm)/Fe(5 nm) ultra-thin layers on GaAs(001) substrate (figure 1(a)) in two stages following the procedure described in a previous publication.²³ The growth of Fe on GaAs is well known and the Fe/GaAs system has been extensively studied²⁴ moreover GaAs has been also chosen as a substrate for a future possible integration of this device in the semiconductor industry. Finally the piezoelectric properties²⁵ of this semiconductor makes it interesting for future piezoelectric/magnetostrictive coupling studies. In the first stage, performed in the molecular beam epitaxy (MBE) chamber of APE beamline at Elettra in Trieste, the surface oxide layer of a commercial undoped GaAs (001) crystal was removed by Ar^+ sputtering. Then, Fe (5 nm) and MgO (2.5 nm) layers were successively grown by e-beam evaporators at room temperature. The Fe epilayer shows an epitaxial relationship with GaAs substrate (Fe (001) out-of-plane orientation and Fe [110] direction along GaAs [110]) while the MgO layer is rotated 45° in-plane with respect to Fe (MgO [100] parallel to Fe [110]). Fe and MgO layers thicknesses were chosen to optimize the tunneling magnetoresistance as described in previous publications.^{19,26} In a second stage, the growth of $\text{Fe}_{1-x}\text{Ga}_x$ films on MgO/Fe/GaAs was performed in a molecular beam epitaxy system at Institut des Nanosciences de Paris. After a heating treatment in UHV for cleaning the samples surface, a $\text{Fe}_{0.8}\text{Ga}_{0.2}$ thin film was deposited by MBE with a growth rate of 0.2 nm per minute and appropriate stoichiometric proportion of the beam equivalent pressures of Fe and Ga.²⁷ The whole heterostructure was finally capped with a protective layer of Au. The top $\text{Fe}_{1-x}\text{Ga}_x$ layer is (001)-oriented with in-plane cubic axes aligned with respect to the Fe bottom layer^{23,27} (figure 1(a)).

After this growing step, the Au/ $\text{Fe}_{0.8}\text{Ga}_{0.2}$ /MgO/Fe/GaAs multilayer was patterned in sets of $20 \times 20 \mu\text{m}^2$ pillars (fig. 1(c)) using a dry etching technique with Ar^+ ions. The pillar regions were first protected by a 150nm-thick Al metallization obtained by standard UV lithography, e-beam evaporation and lift-off. Aluminum was chosen as the mask material because it displays an amphoteric behavior and can be etched by basic solution, while most of alternative masking materials would require an acid attack which is very dangerous for the delicate MgO tunnel barriers of the MTJ. After this lithographic step, the top Au, FeGa, MgO and Fe layers were removed in a plasma etching chamber using 0.3mbar Ar plasma and an input radio-frequency power of 200W. The resulting substrate bias was typically 400V. Etching was performed in a set of about 50-60 times 15 seconds repetitions, with an interval of 15 seconds between consecutive repetitions, in order to minimize sample heating and the possible consequent damage of the multilayer structure. The Al mask was removed at the end of the etching protocol using a TMAH-based solution. An insulating lifting layer was fabricated using UV lithography on SU-8 2002, as a base for the device bonding pads, which need to be electrically insulated from the exposed GaAs regions of the substrate. In order to ensure a smooth interface between the bonding pads and the top of the MTJ pillars, SU-8 was exposed while keeping a gap of about 10 μm between the UV mask and the sample. This yielded a smooth border at the edge of the

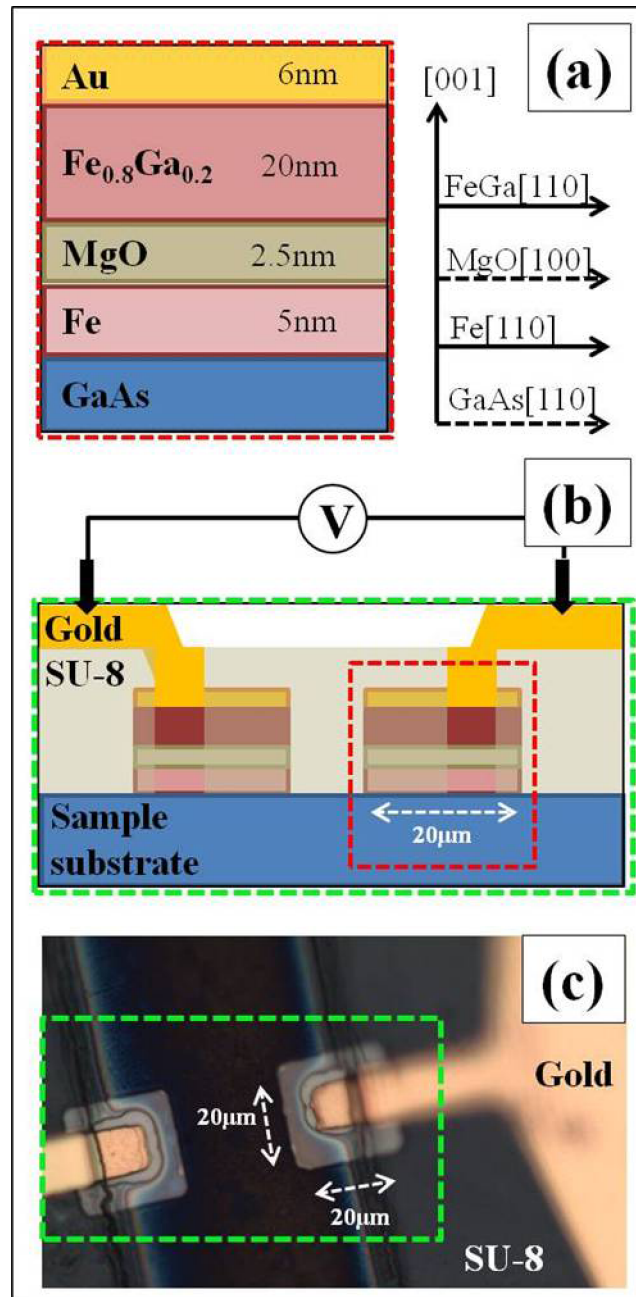


FIG. 1. (a) Description of the multilayer structure and the related epitaxial relationship between the different layers. (b) Scheme of the device and bonding of the sample. The two black arrows indicate the contacts for the electrical measurements. (c) Optical image of a couple of pillars and bonding pads.

exposed SU-8 (see fringes in the optical picture on the left side of Fig. 1(c)). As a final step, bonding pads were obtained by UV lithography, e-beam evaporation of a Ti (10nm)/Au (100nm) bilayer and lift-off. The electrical conduction was ensured on top of these pads by gold wire bonding.

ELECTRICAL MEASUREMENTS

Electrical characterizations were performed through two magnetic tunnel junctions in a symmetric configuration as shown on figure 1(b) (see black arrows). The measurements were performed in a

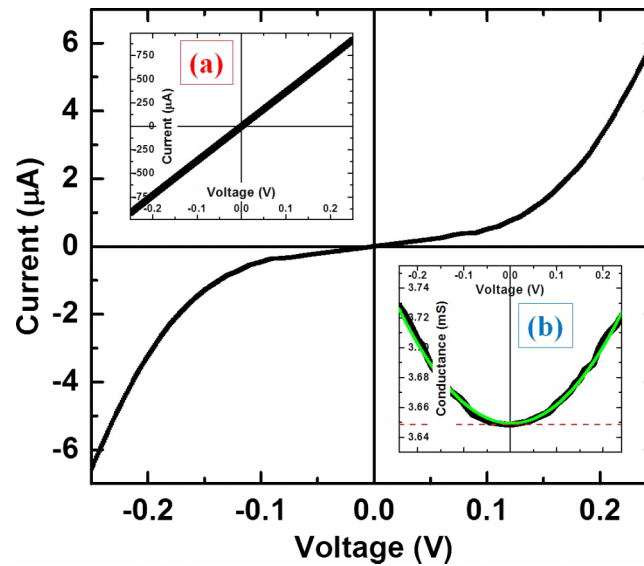


FIG. 2. Voltage dependent tunneling current in the barrier (main panel); I/V curve of the device before any data treatment (top inset [a]); first derivative of the I/V curve (bottom inset [b]) and 2nd order polynomial fit (green). The red dotted line corresponds to a constant conductance due to the ohmic contribution in the current.

two-point mode at room temperature using a Keithley picoammeter/voltage source 6487. The raw I/V curve of these junctions in between $-0.25\text{V} < V < 0.25\text{V}$ is shown in the top inset of figure 2(a) revealing a mainly ohmic behavior with a resistance of 275Ω . Indeed, in the experimental geometry chosen for the electrical measurements, the current is flowing, in between the two junctions, through the GaAs substrate, which, being undoped, has a high resistance that hinders the contribution of the MgO barriers. As a consequence, the high resistance of the substrate is responsible for the mainly ohmic behavior of the current. Nevertheless, the derivative of this I/V curve (figure 2(b)) indicates a non linear contribution which is interpreted^{28,29} to be a current tunneling through the MgO barrier and is reaching 0.4% of the total current at 0.2V. This contribution can be fitted by a second order polynomial curve (green curve on the bottom inset of figure 2(b)) as described in the Brinkman-Dynes-Rowell model³⁰ but the fitted values of thickness and height of the barrier are difficult to interpret due to the specificities of the geometry of our measurements.

In an attempt to evaluate the tunneling contribution, the ohmic contribution has been removed to show only the non-linear contribution represented by the voltage dependence of the tunneling current (main panel in figure 2). The conductance versus voltage curve is interpreted as the sum of a constant conductance (red dotted line on the bottom inset b of figure 2) due to the ohmic contribution and a 2nd order polynomial curve describing the tunneling contribution. The constant conductance contribution has been subtracted and the resulting curve integrated to finally display the current versus voltage behavior of the tunnel barriers (main panel on figure 2).

On this same device, a magnetic field of up to 200 Oe has been applied in the in-plane FeGa[110]||Fe[110] direction.²³ A measurement of the current as a function of magnetic field applied has been performed at a fixed bias voltage of 0.2V. The resulting magnetoresistance curve is finally printed on figure 3 (blue). It shows the magnetoresistance calculated in percentage using the ratio $(R-R_0)/R_0$ with R_0 being the resistance in parallel state of the ferromagnetic layers. On the same graph (black), we show the longitudinal magneto-optical Kerr effect (MOKE) characterization of this sample along the same FeGa[110]||Fe[110] magnetic axis previously done on the continuous thin film heterostructure.²³

As already described (see Reference 23), the hysteresis curve shows a double-step switching process of magnetization in the FeGa/MgO/Fe heterostructure testifying the decoupling between the two ferromagnetic FeGa and Fe layers despite the relatively thin MgO barrier (2.5nm). The first step around 40 Oe corresponds to the bottom Fe layer while the second and complete step around 90 Oe is

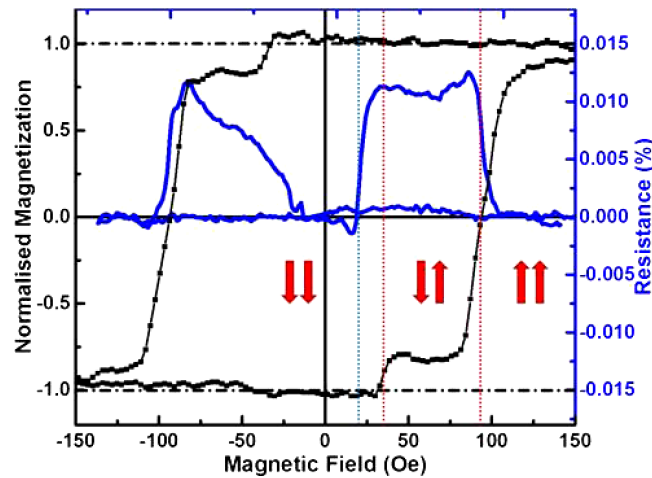


FIG. 3. Hysteresis curve of the heterostructure obtained by MOKE extracted from Ref. 23 (black) and magnetoresistance effect measured after patterning (blue). The red arrows indicate the direction of magnetization of the top FeGa (right arrow) and bottom Fe (left arrow) layers for an increasing magnetic field.

due to the reversal mechanism of the FeGa top layer (red dotted lines on fig. 3). Thus, for an increasing applied magnetic field, between $|40 \text{ Oe}| < H < |90 \text{ Oe}|$, the magnetizations of FeGa top layer and Fe bottom layer are opposite in direction (see arrows representing magnetic field direction in both FM layers for an increasing H from -150 Oe to $+150 \text{ Oe}$). This effect is concomitant with a change of resistance in the pillars of around 0.01% in the same magnetic field range (fig. 3), thus determining an observable magnetoresistance at room temperature.

A close inspection of Figure 3 indicates that the jump in the resistance and the coercive field of the soft ferromagnetic layer do not match perfectly. In fact, the magnetoresistance effect experimentally measured occurs for applied magnetic field $|20 \text{ Oe}| < H < |90 \text{ Oe}|$. One would expect that the increase in resistance appears exactly when the two ferromagnetic layers show magnetization in opposite direction. This observed discrepancy can be mainly attributed to the patterning process which may have damaged the thin Fe bottom layer (5nm). It is especially possible that the etching process have induced structural (defects) and chemical (oxidation) changes at the edges of the pillars changing the coercive field of the whole Fe layer from around 40 Oe to 20 Oe (blue dotted line on fig. 3). On the contrary, the FeGa top layer, which is originally thicker (20nm), has not been affected by the formation of the pillar structure, which explains the unchanged magnetic field of around 90 Oe for the second border of the magnetoresistance effect. The magnetoresistance effect is due to the current tunneling through the MgO barriers. Because the main contribution to the current is ohmic, the overall change of resistance measured is not well representative of the behavior of the junction itself. To evaluate the effective magnetoresistance of the magnetic tunnel junction, we have considered the ratio of magnetoresistance measured being due to a change of current in the only small tunneling contribution, the ohmic main contribution being unchanged in parallel and antiparallel states. This gives us an effective magnetoresistance of up to 11.5% . AlOx barriers have been first considered for building magnetic tunnel junction with a magnetoresistance ratio of up to 70% for example for the CoFeB/AlOx/CoFeB stack.³¹ On the contrary, MgO barrier is well known for giving much higher magnetoresistance ratio like in the CoFeB/MgO/CoFeB junction³² where the ratio can reach 604% . Our own multilayer stack is based on the famous Fe/MgO/Fe junction which was initially reported with a magnetoresistance of 180% by Yuasa and coworker¹⁹ thanks to coherent tunneling of Fe electrons through the MgO barrier. The comparison between this reported value of magnetoresistance in Fe/MgO/Fe MTJ and our result on FeGa/MgO/Fe multilayer stack is clearly an indication of a very small effect.

To explain this great difference in magnetoresistance ratio, we have first to point out the relatively large size of pillar structures used in this study ($20 \times 20 \mu\text{m}^2$) and, as discussed previously on the line shape of the TMR plot, the patterning process that may have damaged the edges of the pillars reducing

the measured TMR. As a consequence, the presence of pin holes or structural defects (inside the pillars or at his edges) is possible and would clearly reduce the quality of the MgO barrier. In addition to this, the insertion of Ga in the top layer may change the electronic properties of one electrode of this MTJ and thus the coherency of the tunneling electrons. However, this change of electronic properties of Fe in FeGa compound was not observed by absorption spectroscopy techniques^{33,34} for a Ga content below 30%. On another side, the introduction of Ga in the top Fe layer may significantly change the interface between the ferromagnetic layer and MgO either by introducing defects due to the complicated growth procedure or because of the intrinsic FeGa/MgO interface architecture (Ga segregation). These parameters could play a detrimental role by lowering the spin polarization. As a consequence, the device patterning process but also the growth mode of galfenol on MgO should be of particular interest and different strategies of growth of the whole multilayer stack have to be considered.

CONCLUSION

We have successfully grown an epitaxial $\text{Fe}_{0.8}\text{Ga}_{0.2}/\text{MgO}/\text{Fe}/\text{GaAs}$ stack by MBE. On this film, we have realized $20 \times 20 \mu\text{m}^2$ -sized pillars by a combination of UV lithography and physical etching.

I/V curves of these devices have shown a mainly ohmic behavior due to the current flowing through the substrate and a non-linear contribution attributed to tunneling current through the MgO barrier. Magnetoresistive characterizations have shown a change of the resistance of the device corresponding to an effective magnetoresistance of 11.5%. This value, which is far below the value reported for the Fe/MgO/Fe MTJ stack, is however large enough to be suitable for application in hybrid devices in which the mechanical stress will be employed to influence the magnetization of the magnetostrictive layer.

ACKNOWLEDGEMENTS

This work has been partly performed in the framework of the new NFFA demonstrator facility on APE beamline. We also acknowledge partial support from ANR (SPINSAW, ANR 13-JS04-0001-01).

- ¹ L. W. Martin and R. Ramesh, *Acta Mater.* **60**, 2449 (2012).
- ² M. Fiebig, *J. Phys. D: Appl. Phys.* **38**, R123 (2005).
- ³ G. Radaelli, D. Petti, E. Plekhanov, I. Fina, P. Torelli, B. R. Salles, M. Cantoni, C. Rinaldi, D. Gutiérrez, G. Panaccione, M. Varela, S. Picozzi, J. Fontcuberta, and R. Bertacco, *Nat. Commun.* **5**, 3404 (2014).
- ⁴ Y. Shiota, T. Nozaki, F. Bonell, S. Murakami, T. Shinjo, and Y. Suzuki, *Nat. Mater.* **11**, 39 (2011).
- ⁵ C. A. F. Vaz, *J. Physics: Condens. Matter* **24**, 333201 (2012).
- ⁶ W. Eerenstein, N. D. Mathur, and J. F. Scott, *Nature* **442**, 759 (2006).
- ⁷ G. Catalan and J. F. Scott, *Adv. Mater.* **21**, 2463 (2009).
- ⁸ Y.-H. Chu, L. W. Martin, M.B. Holcomb, M. Gajek, S.-J. Han, Q. He, N. Balke, C.-H. Yang, D. Lee, W. Hu, Q. Zhan, P.-L. Yang, A. Fraile-Rodríguez, A. Scholl, S.X. Wang, and R. Ramesh, *Nat. Mater.* **7**, 478 (2008).
- ⁹ G. Venkataiah, Y. Shirahata, I. Suzuki, M. Itoh, and T. Taniyama, *J. Appl. Phys.* **111**, 033921 (2012).
- ¹⁰ V. Novosad, Y. Otani, A. Ohsawa, S.G. Kim, K. Fukamichi, J. Koike, K. Maruyama, O. Kitakami, and Y. Shimada, *J. Appl. Phys.* **87**, 6400 (2000).
- ¹¹ Y. Xie, Q. Zhan, Y. Liu, G. Dai, H. Yang, Z. Zuo, B. Chen, B. Wang, Y. Zhang, X. Rong, and R.-W. Li, *AIP Adv.* **4**, 117113 (2014).
- ¹² N. A. Hill, *J. Phys. Chem. B* **104**, 6694 (2000).
- ¹³ M. Löhndorf, S. Dokupil, J. Wecker, M. Rührig, and E. Quandt, *J. Magn. Magn. Mater.* **272-276**, 2023 (2004).
- ¹⁴ A. Tavassolizadeh, P. Hayes, K. Rott, G. Reiss, E. Quandt, and D. Meyners, *J. Magn. Magn. Mater.* (2015).
- ¹⁵ D. Wang, C. Nordman, Z. Qian, J. M. Daughton, and J. Myers, *J. Appl. Phys.* **97**, 10C906 (2005).
- ¹⁶ D. E. Parkes, L. R. Shelford, P. Wadley, V. Holý, M. Wang, a. T. Hindmarch, G. van der Laan, R.P. Campion, K. W. Edmonds, S. a. Cavill, and a. W. Rushforth, *Sci. Rep.* **3**, 2220 (2013).
- ¹⁷ O.M.J. van 't Erve, C.H. Li, G. Kioseoglou, A. T. Hanbicki, M. Osofsky, S.-F. Cheng, and B.T. Jonker, *Appl. Phys. Lett.* **91**, 122515 (2007).
- ¹⁸ J. Atulasimha and A.B. Flatau, *Smart Mater. Struct.* **20**, 043001 (2011).
- ¹⁹ S. Yuasa, T. Nagahama, A. Fukushima, Y. Suzuki, and K. Ando, *Nat. Mater.* **3**, 868 (2004).
- ²⁰ S. Yuasa and D.D. Djayaprawira, *J. Phys. D: Appl. Phys.* **40**, R337 (2007).
- ²¹ W. Butler, X.-G. Zhang, T. Schulthess, and J. MacLaren, *Phys. Rev. B* **63**, 054416 (2001).
- ²² J. Mathon and A. Umerski, *Phys. Rev. B* **63**, 220403 (2001).
- ²³ B. Gobaut, R. Ciprian, B.R. Salles, D. Krizmancic, G. Rossi, G. Panaccione, M. Eddrief, M. Marangolo, and P. Torelli, *J. Magn. Magn. Mater.* **383**, 56 (2015).

- ²⁴ G. Wastlbauer and J.A.C. Bland, *Adv. Phys.* **54**, 137 (2005).
- ²⁵ K. Fricke, *J. Appl. Phys.* **70**, 914 (1991).
- ²⁶ P. Torelli, S. Benedetti, P. Luches, L. Gragnaniello, J. Fujii, and S. Valeri, *Phys. Rev. B* **79**, 035408 (2009).
- ²⁷ M. Eddrief, Y. Zheng, S. Hidki, B. Rache Salles, J. Milano, V.H. Etgens, and M. Marangolo, *Phys. Rev. B* **84**, 161410 (2011).
- ²⁸ P. Torelli, M. Sperl, R. Ciancio, J. Fujii, C. Rinaldi, M. Cantoni, R. Bertacco, M. Utz, D. Bougeard, M. Soda, E. Carlino, G. Rossi, C.H. Back, and G. Panaccione, *Nanotechnology* **23**, 465202 (2012).
- ²⁹ K.M. Bhutta, in *Microsc. Sci. Technol. Appl. Educ.*, edited by A. Méndez-Vilas and J. Díaz (2010), pp. 2022–2027.
- ³⁰ W. F. Brinkman, R. C. Dynes, and J.M. Rowell, *J. Appl. Phys.* **41**, 1915 (1970).
- ³¹ D. Wang, C. Nordman, J.M. Daughton, Z. Qian, and J. Fink, *IEEE Trans. Magn.* **40**, 2269 (2004).
- ³² S. Ikeda, J. Hayakawa, Y. Ashizawa, Y.M. Lee, K. Miura, H. Hasegawa, M. Tsunoda, F. Matsukura, and H. Ohno, *Appl. Phys. Lett.* **93**, 082508 (2008).
- ³³ E. Arenholz, G. van der Laan, A. McClure, and Y. Idzerda, *Phys. Rev. B* **82**, 180405 (2010).
- ³⁴ M. Barturen, M. Sacchi, M. Eddrief, J. Milano, S. Bustingorry, H. Popescu, N. Jaouen, F. Sirotti, and M. Marangolo, *Eur. Phys. J. B* **86**, 191 (2013).